

The lineshape of $\psi(3770)$ and low-lying vector charmonium resonance parameters in $e^+e^- \rightarrow D\bar{D}$

Yuan-Jiang Zhang^{1*}, and Qiang Zhao^{1,2†}

1) *Institute of High Energy Physics, Chinese Academy of Sciences, Beijing 100049, P.R. China and*

2) *Theoretical Physics Center for Science Facilities, CAS, Beijing 100049, P.R. China*

(Dated: February 11, 2019)

We investigate the $D\bar{D}$ production in e^+e^- annihilations near threshold in an effective Lagrangian approach. It shows that the lineshape of the cross section near threshold is sensitive to the contributions from the ψ' though it is below the $D\bar{D}$ threshold. The recent experimental data from BES and Belle collaborations allow us to determine the $\psi'D\bar{D}$ coupling constant which appears to be consistent with other theoretical studies. As a consequence, the ψ' - $\psi(3770)$ mixing parameter can be extracted around the $\psi(3770)$ mass region. Resonance parameters for $\psi(3770)$, $X(3900)$, $\psi(4040)$ and $\psi(4160)$ are also investigated. The $X(3900)$ appears as an enhancement at around 3.9 GeV in the Belle data. In addition to treating it as a resonance, we also study the mechanism that the enhancement is produced by the $D\bar{D}^* + c.c.$ open channel effects. Our result shows that such a possibility cannot be eliminated.

PACS numbers: 13.66.Bc, 12.38.Lg, 14.40.Gx

I. INTRODUCTION

As the first charmonium state above the $D\bar{D}$ threshold, the production of $\psi(3770)$ in $e^+e^- \rightarrow D\bar{D}$ serves as a peculiar probe for exploring the QCD dynamics in the interplay of perturbative and non-perturbative regime. During the past few years experimental measurements were performed at the $\psi(3770)$ region and some interesting observations were exposed. Firstly, BES-II reported a branching ratio for $\psi(3770) \rightarrow \text{non-}D\bar{D}$ up to 15% [1, 2], while CLEO-c found a much smaller non- $D\bar{D}$ branching ratio [3]. Note that so far only one exclusive channel $\psi(3770) \rightarrow \phi\eta$ has been observed in $\psi(3770)$ non-charmonium strong decays. One major concern is how the light hadrons are produced in the $c\bar{c}$ annihilation. In another word, whether this process is dominated by pQCD or there are signs for non-pQCD contributions, is a question for both experiment and theory.

Further interests in this issue are raised by a recent non-relativistic QCD (NRQCD) calculation to the next-to-leading order (NLO) for the $\psi(3770)$ non- $D\bar{D}$ decays [4], where the authors found significant QCD corrections from NLO. Implications of such a result would be that non-pQCD mechanisms may start to play a role. Quantitative studies of non-pQCD mechanisms are presented in Ref. [5, 6], where the authors show that the long-distance interactions due to intermediate D meson loops are essential for understanding the non- $D\bar{D}$ decays of the $\psi(3770)$. This also suggests that a dynamic understanding of the correlation between the $\psi(3770)$ non- $D\bar{D}$ decay and the so-called Okubo-Zweig-Iizuka (OZI)-rule [7]-evading mechanism is required.

The $\psi(3770)$ production in e^+e^- annihilation is also useful for further studying the properties of the $\psi(3770)$. As shown by BES measurement [8, 9], an obvious deviation of the resonance excitations from Breit-Wigner is observed in $e^+e^- \rightarrow D\bar{D}$. This raises the question about the sources of causing such a deviation, and the role played by background processes [10]. One possibility is that some new structures in the energy region between 2.70 and 3.87 GeV may cause such a line shape anomaly [9]. Above the $\psi(3770)$ mass, the data from Belle collaboration suggests an enhancement around 3.9 GeV [11], which

* E-mail: yjzhang@ihep.ac.cn

† E-mail: zhaoq@ihep.ac.cn

could be a signal for resonance. Note that 3.9 GeV is at the open channel threshold for $D\bar{D}^* + c.c.$. Thus, it would be interesting to investigate the $D\bar{D}^* + c.c.$ open channel effects and compare them with the Breit-Wigner solution in the numerical fits. By clarifying these issues in both experiment and theory we expect that the $\psi(3770)$ resonance parameters can be determined. Furthermore, the recent controversial results from BESII [1, 2] and CLEO-c [3] on the $\psi(3770)$ non- $D\bar{D}$ decays can be disentangled [5, 6].

In this work we will study the lineshape of $e^+e^- \rightarrow D\bar{D}$ cross section in an effective Lagrangian approach. We will show that the cross section experiences important interferences from the ψ' which will account for the $\psi(3770)$ lineshape deviation from the Breit-Wigner form. A recent analysis of this issue is also done by Ref. [12]. In our work, we will show that the near threshold cross sections is not only to provide evidence for the ψ' - $\psi(3770)$ interferences, but also provide a peculiar constraint on the dynamics for ψ' couplings to the $D\bar{D}$. By determining the $g_{\psi'D\bar{D}}$ coupling, we can then examine the $\psi(2S)$ - $\psi(1D)$ mixing for the ψ' and $\psi(3770)$, and extract the mixing angle at the mass of the $\psi(3770)$ [5, 13]. We will study the energy-dependence of the mixing parameter. It is essential to keep unitarity, and further dynamical information about the state evolutions could be gained.

We will also investigate the bump around 3.9 GeV observed by Belle [11]. Given the success of the potential quark model (see Ref. [14] for a recent review), a vector charmonium with $J^{PC} = 1^{--}$ at 3.9 GeV will bring great concerns on the non-relativistic $c\bar{c}$ phenomenology. We will show that this enhancement may be caused by the $D\bar{D}^* + c.c.$ open channel effects.

This work is organized as follows: In Sect. II, we formulate the transition amplitudes for $e^+e^- \rightarrow D\bar{D}$ from different sources, which include charmonium resonance excitations, electromagnetic (EM) background from vector meson dominance (VMD) model and open $D\bar{D}^* + c.c.$ effects via intermediate meson loops. In Sect. III, we present our numerical results along with experimental observables. A summary will be given in Sect. IV.

II. THE MODEL

The ingredients considered in this work include charmonium resonance excitations and electromagnetic (EM) background (Fig. 1), and open-charm effects via intermediate meson loops (Fig. 2). The charmonium resonance excitations are constructed in the VMD model [15–17], where the EM field will be decomposed into vector meson fields with both isospin 0 and 1 components. By taking away explicitly the nearby resonance contributions from e.g. $\psi(3770)$ and ψ' , the EM background contributions arising from the continuum part can thus be parameterized by an effective coupling and minimized in the numerical fit.

We also examine the $D\bar{D}$ final state interactions in $e^+e^- \rightarrow \gamma^* \rightarrow \psi' \rightarrow (D\bar{D}, D\bar{D}^* + c.c., D^*\bar{D}^*) \rightarrow D\bar{D}$ due to intermediate $D\bar{D}$, $D\bar{D}^* + c.c.$, and $D^*\bar{D}^*$ meson loops as shown in Fig. 2. These contributions are not double-counting the ψ' excitation in Fig. 1 since a Breit-Wigner is explicitly introduced there. The effects of such a loop contribution may give rise to both energy-dependence of the ψ' total width and a relative phase to the QED diagram. However, we note in advance that these contributions are negligibly small. It also should be clarified that there is no need to consider the intermediate meson loop contributions for $\psi(3770)$ since the effective coupling $g_{\psi(3770)D\bar{D}}$ is extracted from experimental data and should have included the loop effects.

To study the $D\bar{D}^* + c.c.$ open channel effects, we apply the experimental data for $e^+e^- \rightarrow D\bar{D}^* + c.c.$ from Belle [18]. This is equivalent to isolating out the $D\bar{D}^* + c.c.$ open channel contributions from all possible sources, and can be compared with the Breit-Wigner fit.

In order to evaluate the diagrams of Figs. 1 and 2, the following effective Lagrangians are needed:

$$\begin{aligned}
\mathcal{L}_{V D \bar{D}} &= g_{V D \bar{D}} \{ D \partial_\mu \bar{D} - \partial_\mu D \bar{D} \} \mathcal{V}^\mu, \\
\mathcal{L}_{V D \bar{D}^*} &= -i g_{V D \bar{D}^*} \epsilon_{\alpha\beta\mu\nu} \partial^\alpha \mathcal{V}^\beta \partial^\mu \bar{D}^{*\nu} D + h.c., \\
\mathcal{L}_{\mathcal{P} D^* \bar{D}^*} &= -i g_{\mathcal{P} D^* \bar{D}^*} \epsilon_{\alpha\beta\mu\nu} \partial^\alpha \mathcal{P}^{\beta} \partial^\mu \bar{D}^{*\nu} \mathcal{P} + h.c., \\
\mathcal{L}_{\mathcal{P} \bar{D} D^*} &= g_{D^* \mathcal{P} \bar{D}} \{ \bar{D} \partial_\mu \mathcal{P} - \partial_\mu \bar{D} \mathcal{P} \} \mathcal{D}^{*\mu}, \\
\mathcal{L}_{V D^* \bar{D}^*} &= g_{V D^* \bar{D}^*} \mathcal{V}^\mu [(D^{*\nu} \overleftrightarrow{\partial}_\mu \bar{D}_\nu^* - D^{*\nu} \overleftarrow{\partial}_\mu \bar{D}_\nu^*) - D^{*\nu} \overrightarrow{\partial}_\nu \bar{D}_\mu^* + D^{*\mu} \overleftarrow{\partial}_\nu \bar{D}_\nu^*],
\end{aligned} \tag{1}$$

where \mathcal{P} and \mathcal{V} are the pseudoscalar and vector mesons, and $\epsilon_{\alpha\beta\mu\nu}$ is the antisymmetric tensor.

A. Charmonium excitations in VMD and EM background contribution

According to VMD [15, 16], the EM current can be decomposed into two parts. One is hadronic part containing a complete sum over all isospin-0 and 1 vector meson fields, while the other is so-called “bare photon” field. An empirical role played by the EM “bare photon” field is to assure the proper normalization of the physical photon field. Its contribution is generally small. Therefore, this part is minimized in the VMD model.

In reality, it is not possible to include all hadronic vector meson amplitudes. A commonly adopted way is to include the vector meson resonances in the vicinity of the considered kinematics, and then treat the unknown part as an EM background which now includes the off-shell contributions from those far away resonances and the “bare photon” amplitude. This would also be our strategy here to apply the VMD model to $e^+e^- \rightarrow D\bar{D}$ near threshold. In Fig. 1, diagram (a) and (b) demonstrate the hadronic contributions and the EM background, respectively.

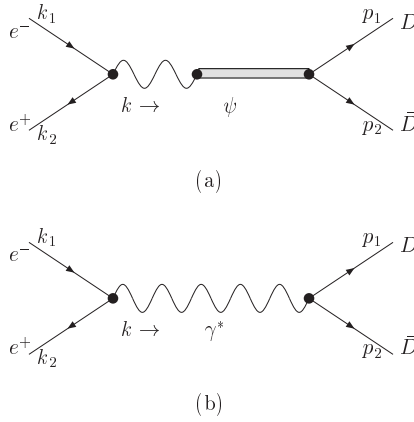


FIG. 1: Feynman diagrams based on the VMD model for $e^+e^- \rightarrow D\bar{D}$ near threshold. Diagram (a) is for hadronic vector meson contributions, while (b) represents the EM background.

Setting $m_e \simeq 0$, the coupling of vector mesons with the virtual photon can be extracted from experimental data by the VMD model [16, 17]:

$$\frac{e}{f_\psi} = \left[\frac{3\Gamma_{\psi \rightarrow e^+e^-}}{2\alpha_e |\vec{p}_e|} \right]^{1/2}, \quad (2)$$

where $|\vec{p}_e|$ is the electron three-momentum in the vector meson rest frame, $\Gamma_{\psi \rightarrow e^+e^-}$ is the partial decay width, and $\alpha_e = 1/137$ is the fine-structure constant.

The amplitude of Fig. 1(a) due to ψ resonance excitations can be written as:

$$T_a = e^2 \bar{v}(k_2) \gamma_\mu u(k_1) \frac{1}{s} \frac{m_\psi^2}{f_\psi} \frac{1}{s - m_\psi^2 + im_\psi \Gamma_\psi} g_{\psi D\bar{D}} (p_1 - p_2)^\mu, \quad (3)$$

where Γ_ψ is the total width of the charmonium resonance, and $u(k_1)$ and $v(k_2)$ are the Dirac spinors for the electron and positron, respectively; The four vectors p_1 and p_2 are the momenta for the final state D and \bar{D} meson.

We parameterize the EM background contributions to $e^+e^- \rightarrow D\bar{D}$ as follows:

$$T_b = e^2 \bar{v}(k_2) \gamma_\mu u(k_1) \frac{1}{s} g_c(s) (p_1 - p_2)^\mu, \quad (4)$$

where g_c is an effective coupling of the EM background contribution to $D\bar{D}$. As pointed earlier, this amplitude contains the “bare photon” contribution and contributions from other vectors which are not

explicitly included. In this sense, the value for g_c will depend on how many vector charmonium states are included in the fitting. The inclusion of more higher states near threshold will minimize this amplitude.

Combining Eqs. (3) and (4), one obtains the total amplitude for $e^+e^- \rightarrow D\bar{D}$

$$T = \frac{e^2 \bar{v}(k_2) \gamma_\mu u(k_1) (p_1 - p_2)^\mu}{s} [g_c(s) + \frac{m_{\psi'}^2}{f_{\psi'}} \frac{g_{\psi' D\bar{D}}}{s - m_{\psi'}^2 + im_{\psi'} \Gamma_{\psi'}} + \sum_{\psi_i} \frac{m_{\psi_i}^2}{f_{\psi_i}} \frac{g_{\psi_i D\bar{D}}}{s - m_{\psi_i}^2 + im_{\psi_i} \Gamma_{\psi_i}} e^{i\phi_i}], \quad (5)$$

where the ψ' amplitude is explicitly included, and a phase factor $e^{i\phi_i}$ is added to other charmonium resonance amplitudes above the $D\bar{D}$ threshold. Then, the cross section for $e^+e^- \rightarrow D\bar{D}$ can be written as

$$\sigma(e^+e^- \rightarrow D\bar{D}) = \frac{8\pi\alpha_e^2 |\vec{p}|^3}{3 s^{5/2}} |g_c(s) + \frac{m_{\psi'}^2}{f_{\psi'}} \frac{g_{\psi' D\bar{D}}}{s - m_{\psi'}^2 + im_{\psi'} \Gamma_{\psi'}} + \sum_{\psi_i} \frac{m_{\psi_i}^2}{f_{\psi_i}} \frac{g_{\psi_i D\bar{D}}}{s - m_{\psi_i}^2 + im_{\psi_i} \Gamma_{\psi_i}} e^{i\phi_i}|^2, \quad (6)$$

where $|\vec{p}|$ is the D -meson three-vector momentum in the overall c.m. frame.

B. Intermediate meson loop contributions and $D\bar{D}^* + c.c.$ open channel effects

The intermediate meson loops via the $D\bar{D}$, $D\bar{D}^* + c.c.$ and $D^* \bar{D}^*$ rescatterings in Fig. 2 can be evaluated as follows [5, 19]:

$$T_L = -ie^2 \bar{v}(k_2) \gamma_\mu u(k_1) \frac{1}{s} \frac{m_\psi^2}{f_\psi} \frac{1}{s - m_\psi^2 + im_\psi \Gamma_\psi} \int \frac{d^4 p_2}{(2\pi)^4} \sum_{\text{polarization}} \frac{T_1 T_2 T_3}{a_1 a_2 a_3} \mathcal{F}(p_2^2). \quad (7)$$

Taking $D\bar{D}(\rho)$ as a example, the vertex functions for the $D\bar{D}(\rho)$ loop are

$$\begin{cases} T_1 \equiv ig_1(l_1 - l_3) \cdot \varepsilon_\psi \\ T_2 \equiv ig_2(l_1 + p_1) \cdot \varepsilon_\rho \\ T_3 \equiv ig_3(l_3 + p_2) \cdot \varepsilon_\rho^* \end{cases} \quad (8)$$

where g_1 , g_2 , and g_3 are the coupling constants at the meson interaction vertices (see Fig. 2). The four-vector momentum, l_1 , l_2 , and l_3 are for the intermediate mesons, respectively, while $a_1 = l_1^2 - m_1^2$, $a_2 = l_2^2 - m_2^2$, and $a_3 = l_3^2 - m_3^2$ are the denominators of the propagators of intermediate mesons.

Divergences are inevitable in the loop integrals. Since the effective Lagrangian approach is not a renormalizable theory, a common way to kill the divergences is to introduce a form factor as a cut-off for those unphysical contributions from the ultra-violet regime. Such a prescription will also compensate the internal particle off-shell effects. The form factor $\mathcal{F}(p^2)$ is usually parameterized as

$$\mathcal{F}(p^2) = \left(\frac{\Lambda^2 - m_{ex}^2}{\Lambda^2 - p^2} \right)^n, \quad (9)$$

where $n = 0, 1, 2$ correspond to different treatments of the loop integrals. If the on-shell approximation is applicable [20–22], the loop integrals will not suffer from the divergences, and the form factor will take care of the off-shell effects. In the present work, we consider the dipole form factor, i.e. $n = 2$, in the full loop integral. The cut-off energy Λ is usually parameterized as

$$\Lambda = m_{ex} + \alpha \Lambda_{QCD}, \quad (10)$$

where $\Lambda_{QCD} = 220$ MeV and α is a tunable parameter, and m_{ex} is the mass of the exchanged meson. There are different expressions for the form factor adopted in the literature. However, note that the cut-off is always tunable. We would generally need experimental data to determine a proper form factor parameter.

The charmed meson couplings to the light mesons are obtained in the chiral and heavy quark limits [23],

$$\begin{aligned} g_{D^*D\pi} &= \frac{2}{f_\pi} g \sqrt{m_D m_{D^*}}, & g_{D^*D^*\pi} &= \frac{g_{D^*D\pi}}{\tilde{M}_D}, \\ g_{D^*D\rho} &= \sqrt{2}\lambda g_\rho, & g_{DD\rho} &= g_{D^*D\rho} \tilde{M}_D, \end{aligned} \quad (11)$$

with $f_\pi = 132$ MeV, and $\tilde{M}_D \equiv \sqrt{m_D m_{D^*}}$ is a mass scale. The parameters g_ρ respects the relation $g_\rho = m_\rho/f_\pi$ [24]. We take $\lambda = 0.56 \text{ GeV}^{-1}$ and $g = 0.59$ [25].

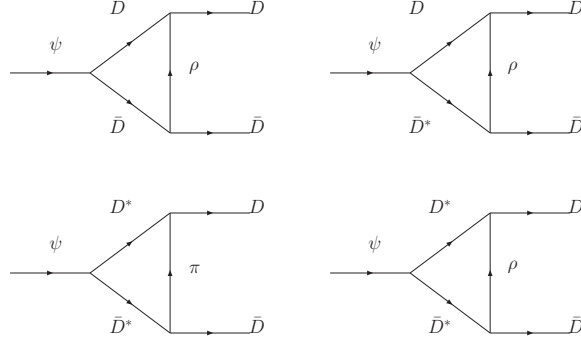


FIG. 2: Feynman diagrams for intermediate meson loops as corrections for the $D\bar{D}$ coupling to a charmonium state.

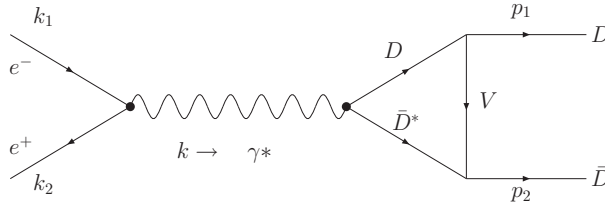


FIG. 3: Feynman diagram for the $D\bar{D}^* + c.c.$ open channel effects.

The $D\bar{D}^* + c.c.$ open channel effects (see Fig. 3) can be calculated in a similar way. The experimental data from Belle for $e^+e^- \rightarrow D\bar{D}^* + c.c.$ [18] will allow us to extract the $\gamma^* D\bar{D}^*$ coupling $g_{\gamma^* D\bar{D}^*}(s)$ [19]:

$$\sigma(e^+e^- \rightarrow D\bar{D}^* + c.c.) = \frac{4\pi}{3} \frac{|\vec{p}|^3}{s^{3/2}} \alpha_e^2 |g_{\gamma^* D\bar{D}^*}(s)|^2, \quad (12)$$

where $|\vec{p}|$ is the D -meson three-vector momentum in the overall c.m. frame.

As briefly mentioned earlier, explicitly adopting the experimental data for $e^+e^- \rightarrow D\bar{D}^* + c.c.$ means that all the resonances which can couple to $D\bar{D}^* + c.c.$ are included in the effective coupling form factor $g_{\gamma^* D\bar{D}^*}(s)$. This will lead to double-counting with the treatment of explicitly including $\psi(3770)$ and other resonances. Because of this ambiguity we will only calculate the exclusive open channel contributions in the following section, and discuss its behavior around the open channel kinematics.

C. The ψ' - $\psi(3770)$ mixing

The nonvanishing $g_{\psi'D\bar{D}}$ extracted from the cross section measurement will allow us to investigate the ψ' - $\psi(3770)$ mixing. As a dynamic consequence of the intermediate $D\bar{D}$ loop (and $D\bar{D}^* + c.c.$ etc), such a higher order effect can be quantified in $e^+e^- \rightarrow D\bar{D}$.

For a two-state $\psi' - \psi(3770)$ mixing, the covariant propagator can be expressed as [26, 27]:

$$G = \frac{1}{D_{\psi'} D_{\psi(3770)} - |D_{\psi'\psi(3770)}|^2} \begin{pmatrix} D_{\psi'} & D_{\psi'\psi(3770)} \\ D_{\psi'\psi(3770)} & D_{\psi(3770)} \end{pmatrix}, \quad (13)$$

where $D_{\psi'}$ and $D_{\psi(3770)}$ are the denominators for the propagators of ψ' and $\psi(3770)$:

$$D_i = s - m_i^2 + i\sqrt{s} \Gamma_i(s), \quad (14)$$

with the energy-dependent width

$$\Gamma_i(s) = \frac{1}{6\pi s} [g_{\psi_i D^+ D^-}^2 |\vec{p}_{D^+}(s)|^3 + g_{\psi_i D^0 \bar{D}^0}^2 |\vec{p}_{D^0}(s)|^3 + \dots] + \Gamma_{\psi_i}^{\text{non-}D\bar{D}}, \quad (15)$$

dominated by the $D\bar{D}$ channel near the $\psi(3770)$ mass region. $|\vec{p}_i(s)| = \sqrt{s - 4m_i^2}/2$ is the three-vector momentum carried by the intermediate D meson at an energy \sqrt{s} .

The $D_{\psi'\psi(3770)}$ is the mixing term via the $D\bar{D}$ meson loop:

$$D_{\psi'\psi(3770)} = \frac{1}{6\pi\sqrt{s}} [g_{\psi' D^+ D^-} g_{\psi(3770) D^+ D^-} |\vec{p}_{D^+}(s)|^3 + g_{\psi' D^0 \bar{D}^0} g_{\psi(3770) D^0 \bar{D}^0} |\vec{p}_{D^0}(s)|^3 + \dots], \quad (16)$$

from which we can define the mixing parameter $|\xi|$:

$$|\xi_i| \equiv \left| \frac{D_{\psi'\psi(3770)}}{D_i} \right|. \quad (17)$$

Several points should be made: (i) In the energy region near the $\psi(3770)$ mass (below the $D\bar{D}^* + c.c.$ open channel), the $D\bar{D}$ loop is the dominant contribution to the mixing matrix element. We restrict the discussion in this region and neglect the contributions from the $D\bar{D}^* + c.c.$ and other high threshold loops. But we mention that contributions from the $D\bar{D}^* + c.c.$ loop is rather small when \sqrt{s} is above the threshold. (ii) In principle, the vertex couplings $g_{\psi' D\bar{D}}$ and $g_{\psi(3770) D\bar{D}}$ should be s -independent in Eq. (9). In our case, the $g_{\psi' D\bar{D}}$ is extracted by fitting the cross section data, and no obvious s -dependence is needed within the energy region near threshold. We thus adopt a constant coupling here. Nevertheless, it shows that the s -dependence of the total width $\Gamma_i(s)$ is also weak. This justifies that the mixing parameter extracted above is at an accuracy of leading order. (iii) In Eq. (15) the non- $D\bar{D}$ channel contributions to the total width are rather small due to much weaker couplings. As a leading order estimate we apply the PDG values to fix these two widths and do not consider their s -dependence, i.e. $\Gamma_{\psi'}^{\text{non-}D\bar{D}} = 317 \text{ KeV}$ and $\Gamma_{\psi(3770)}^{\text{non-}D\bar{D}} = 4.15 \text{ MeV}$ [28].

III. NUMERICAL RESULTS

Proceeding to the numerical calculation, our fitting strategy is to minimize the background contributions given that the necessary resonance amplitudes are included. We thus perform two separate fits of the data. One is restricted to the near threshold region (Fit-I) and the other is extended to $\sqrt{s} \simeq 4.3 \text{ GeV}$ covered by the Belle data [11] (Fit-II). This separate treatment is based on the different experimental situations between BES and Belle. BES has a relatively detailed scan over the energy region from threshold to the upper end of the $\psi(3770)$ mass, while the energy bins in Belle data are much larger and the cross sections have larger uncertainties. Moreover, the Belle data are extracted from the exclusive initial state radiation (ISR) production of $D\bar{D}$ at c.m. energy 10.58 GeV, and are corrected by the ISR. The advantage of the Belle data is that they cover nearly the whole energies from threshold up to $\sim 5 \text{ GeV}$.

TABLE I: Fitting parameters for $e^+e^- \rightarrow D^0\bar{D}^0$ and $e^+e^- \rightarrow D^+D^-$ near threshold. The experimental data are from BES [8].

	$e^+e^- \rightarrow D^0\bar{D}^0$	$e^+e^- \rightarrow D^+D^-$
$g_{\psi'D\bar{D}}$	9.05 ± 2.34	7.72 ± 1.02
$g_{\psi(3770)D\bar{D}}$	13.58 ± 1.07	10.71 ± 1.75
$m_{\psi(3770)}$ (MeV)	3774.0 ± 1.3	3774.0 ± 1.6
$\Gamma_{\psi(3770)}$ (MeV)	28.4 ± 2.9	29.6 ± 2.9
ϕ	$228.1^\circ \pm 18.6^\circ$	$190.6^\circ \pm 21.1^\circ$
$\chi^2/\text{d.o.f}$	12.28/9	13.32/9

A. Fit-I

Quantum mechanically, the most important contributions to the $e^+e^- \rightarrow D\bar{D}$ cross sections near threshold would come from the nearby vector charmonia, i.e. $\psi(3770)$ and ψ' . Although ψ' is below the $D\bar{D}$ threshold, its mass is not located far away. Thus, its off-shell contribution may still be sizeable. Since the ψ' has a well-defined mass position and total width, we then fix these two quantities in the analysis, but leave its coupling to $D\bar{D}$ to be fitted by data.

Other fitting parameters include the mass and total width of $\psi(3770)$, the $\psi(3770)D\bar{D}$ coupling, and the relative phase angle between the $\psi(3770)$ and ψ' amplitude. By fitting these parameters to the BES data [8], we actually minimize the contributions from the other resonances and “bare photon”. In Tab. I, the fitting results for $e^+e^- \rightarrow D^0\bar{D}^0$ and $e^+e^- \rightarrow D^+D^-$ are listed separately. It shows that the values of χ^2 are compatible in these two channels. Interestingly, the extracted couplings $g_{\psi'D\bar{D}}$ and $g_{\psi(3770)D\bar{D}}$ appear to have significant differences in the charged and neutral channel. As a comparison, if we extract $g_{\psi(3770)D\bar{D}}$ by the PDG data [28], we obtain $g_{\psi(3770)D^0\bar{D}^0} = 12.43$ and $g_{\psi(3770)D^+D^-} = 12.89$, which are apparently different from the fitted values. In particular, the BES data suggest a relatively larger $g_{\psi(3770)D^0\bar{D}^0}$ coupling than $g_{\psi(3770)D^+D^-}$. We note that in both charged and neutral channel, the fitted mass and total width of $\psi(3770)$ are consistent with each other. It is also interesting to note that the extracted values for $g_{\psi'D\bar{D}}$ are within the range by other approaches [29–32].

In Fig. 4, the fitting results for both channels are presented. The short-dashed curves are exclusive $\psi(3770)$ cross sections while the long-dashed curves are exclusive ψ' . The solid curves are given by the interfering amplitudes between $\psi(3770)$ and ψ' with the relative phase angle $\phi = 228.1^\circ$ and 190.6° for the neutral and charged channel, respectively. Apart from the coupling differences, the differences between the phase angles also contribute to the interferences significantly.

As an estimate of higher resonance effects, we take the PDG average of the total width and the upper limit of the branching ratio $\text{Br}(\psi(4040) \rightarrow D\bar{D}) < 0.2\%$ [28] to extract $g_{\psi(4040)D\bar{D}} \approx 0.34$. The $\psi(4040)$ decay constant can also be extracted from the experimental data by Eq. (2), which gives $e/f_{\psi(4040)} = 9.35 \times 10^{-3}$. In Fig. 4 the exclusive cross sections from $\psi(4040)$ are presented by the dotted curves, which turn out to be negligible near threshold. This justifies the treatment that the cross sections from threshold to the upper end of the $\psi(3770)$ mass are dominated by $\psi(3770)$ and ψ' interferences, and the background contributions (here, they are referred to the “bare photon” and higher resonances) are minimized.

We also calculate the energy-dependence of the cross section ratio between $e^+e^- \rightarrow D^+D^-$ and $e^+e^- \rightarrow D^0\bar{D}^0$ in Fig. 5 to compare with the BES data. It shows an overall agreement except that we should give a caution that the ratio may start to deviate from reality at higher energies since other resonances and mechanisms would start to have stronger interferences. Since the cross sections appear to be sensitive to tiny discrepancies between the charged and neutral channel, a more precise measurement of this quantity would be useful for understanding the underlying mechanisms.

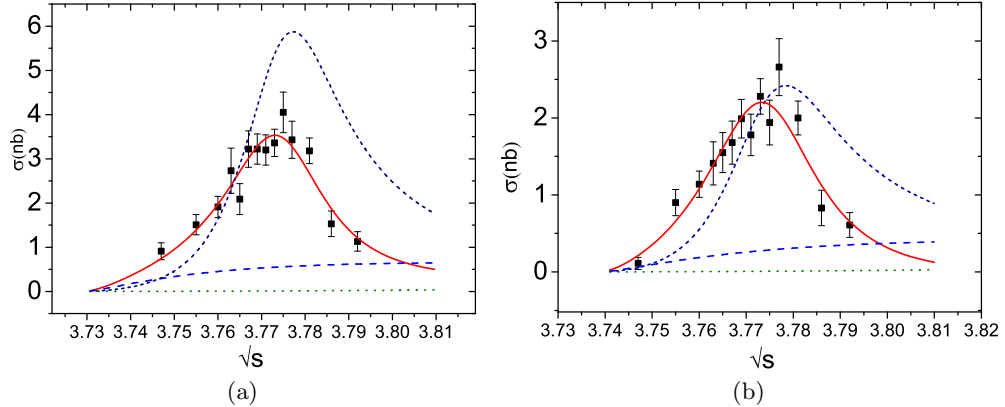


FIG. 4: The cross sections for $e^+e^- \rightarrow D^0\bar{D}^0$ (left) and $e^+e^- \rightarrow D^+D^-$ (right) fitted by the ψ' and $\psi(3770)$ interferences (solid line). The shot-dash line stands for the exclusive $\psi(3770)$ cross section, while dashed line denotes the one for ψ' . The dotted line represents the exclusive contribution from $\psi(4040)$. The data are from BES [8].

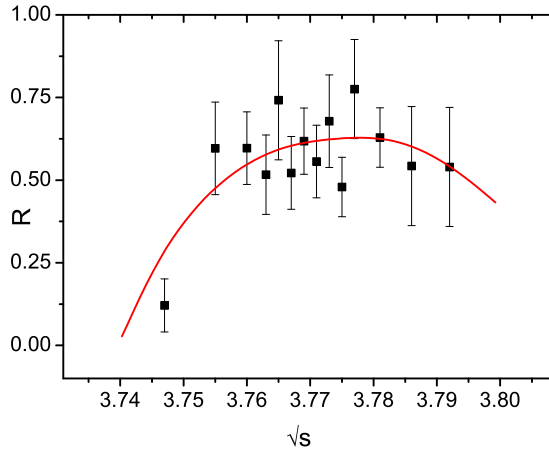


FIG. 5: The cross section ratio between $e^+e^- \rightarrow D^+D^-$ and $e^+e^- \rightarrow D^0\bar{D}^0$ versus c.m. energy \sqrt{s} . The data are from BES [8].

B. Fit-II

In this subsection, we fit the experimental data from Belle [11] by including higher resonances. Apart from $\psi(4040)$ and $\psi(4160)$ from PDG [28], we also include a new state $X(3900)$ in the fit. As shown by the Belle data for $e^+e^- \rightarrow D^0\bar{D}^0$ [11], an enhancement is observed at about 3.9 GeV which could be signals for a charmonium state. Although we fit the data using a Breit-Wigner here, we shall argue later that this enhancement may be due to the $D\bar{D}^* + c.c.$ open channel effects.

The strategy is similar to Fit-I. Namely, we fix the mass and total width of the ψ' and then leave $g_{\psi'D^0\bar{D}^0}$ to be fitted by data. The other fitted quantities include the resonance parameters for $\psi(3770)$, $X(3900)$, $\psi(4040)$, $\psi(4160)$, and their relative phase angles to the ψ' amplitude. In Tab. II, the fitting results are listed and can be compared with Tab. I.

It shows that the coupling $g_{\psi'D^0\bar{D}^0}$ appears to be stable in this fit, while parameters for $\psi(3770)$ exhibit strong sensitivities to the data. In particular, the total width becomes rather small which is even smaller than the PDG average [28]. The phase angle also changes, and the overall effects are that the

TABLE II: Fitting parameters from Fit-II. The results are obtained by fitting the Belle data [11] for $e^+e^- \rightarrow D^0\bar{D}^0$. We separately list the other two fitted quantities here: $g_{\psi'D^0\bar{D}^0} = 9.05 \pm 0.37$, $g_{\psi(3770)D^0\bar{D}^0} = 13.13 \pm 0.65$. The reduced χ^2 is $\chi^2/\text{d.o.f} = 17.45/19$.

	M (GeV)	Γ (MeV)	$g_{VDD}/f_V(\times 10^{-2})$	ϕ
$X(3900)$	3.894 ± 0.011	89.8 ± 12.6	6.76 ± 0.89	$104.36^\circ \pm 7.90^\circ$
$\psi(3770)$	3.7724 ± 0.002	25.4 ± 1.4	23.2 ± 1.1	$198.85^\circ \pm 4.19^\circ$
$\psi(4040)$	4.0812 ± 0.008	96.2 ± 11.4	3.48 ± 0.34	$101.16^\circ \pm 11.742^\circ$

cross sections at the $\psi(3770)$ mass are increased. Such a dramatic change is likely due to the significant discrepancies between the BES and Belle data. Again, a detailed scan over the threshold region is strongly required. The fitted total widths for $X(3900)$ and $\psi(4040)$ turn out to have large uncertainties.

We plot the fitting results in Fig. 6, which appear to be in a good agreement with the Belle data. In comparison with Fit-I, the importance of ψ' is consistently highlighted. Exclusive cross sections from other resonances are also presented in Fig. 6. We note that the smooth-out behavior at the high energy end is favored by the minimization, and it leads to a negligibly small contributions from $\psi(4160)$. Note that the data still have rather large uncertainties. The contributions from $\psi(4160)$ should be restudies with high-quality data. We would not discuss much about it here.

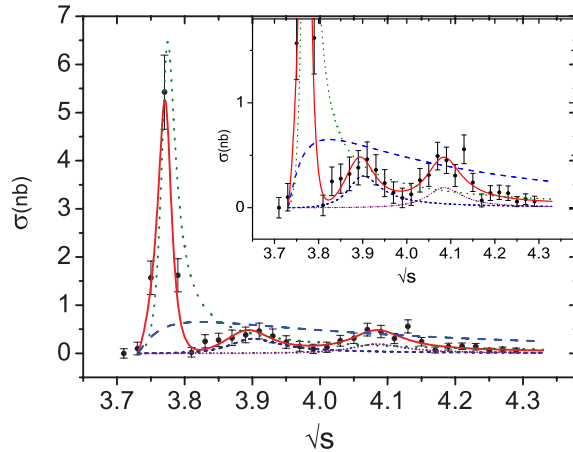


FIG. 6: The Belle cross section for $e^+e^- \rightarrow D^0\bar{D}^0$ [11] fitted by Fit-II. The solid line represents the overall results; the long dashed line denotes the exclusive contribution from ψ' , while the long-dotted, short-dashed and short-dotted lines denote the exclusive cross sections from $\psi(3770)$, $X(3900)$ and $\psi(4040)$, respectively.

C. The $D\bar{D}^* + c.c.$ open channel effects

The enhancement at 3.9 GeV from the Belle data, if is due to resonance excitation, may cause some confusions with the potential model predictions [14] for the charmonium spectrum since one would not expect a $J^{PC} = 1^{--}$ state at this mass region. Taking into account the success of potential quark model, an alternative explanation for this structure would be due to the $D\bar{D}^* + c.c.$ open channel effects as illustrated by Fig. 3.

With the help of Eq. (12) and experimental data for $e^+e^- \rightarrow D^+D^{*-} + c.c.$ from Belle [18], the effective coupling $g_{\gamma^*D\bar{D}^*}(s)$ can be extracted. The corresponding datum points are plotted in Fig. 7 in terms of x ($\equiv s - (m_D + m_{D^*})^2$).

We employ two methods to extract the effective coupling form factor:

- (i) Form factor one (FF-I)

TABLE III: Parameters fitted with FF-I and FF-II for the $\gamma^* D\bar{D}^*$ effective coupling form factor. The data are from Belle [18].

FF-I		FF-II	
$g_{\gamma^* D\bar{D}^*} = g_1 \exp[-(s - (m_D + m_{D^*})^2)/t_1] + g_0$		$g_{\gamma^* D\bar{D}^*} = \left \frac{b_0}{s - m_X^2 + im_X \Gamma_X} + b_1 \right $	
g_1	8.86 ± 0.59	b_0	3.08 ± 0.31
t_1	1.28 ± 0.06	m_X (GeV)	3.943 ± 0.014
g_0	0.43 ± 0.02	Γ_X (MeV)	119.0 ± 10.0
		b_1	0.016 ± 0.045
$\chi^2/\text{d.o.f}$	68.86/53	$\chi^2/\text{d.o.f}$	47.67/52

In FF-I scheme, we fit the data in Fig. 7 by an exponential function:

$$g_{\gamma^* D\bar{D}^*}(s) = g_1 \exp[-(s - (m_D + m_{D^*})^2)/t_1] + g_0, \quad (18)$$

where $x = 0$ corresponds to the $D\bar{D}^* + c.c.$ threshold, and g_1 , t_1 , and g_0 are fitting parameters. The above function can perfectly describe the energy-dependence of the effective coupling. By simply extrapolating the exponential to the $D\bar{D}$ threshold (dashed line in Fig. 7), we then apply this form factor to calculate the open channel cross sections.

(ii) Form factor two (FF-II)

In FF-II scheme, we fit the data in Fig. 7 by a single resonance:

$$g_{\gamma^* D\bar{D}^*}(s) = \left| \frac{b_0}{s - m_X^2 + im_X \Gamma_X} + b_1 \right|, \quad (19)$$

with a background term b_1 . The parameter b_0 can be regarded as the product of the $\gamma^* X$ coupling and $X D\bar{D}^*$ coupling. This parametrization agrees with the data at higher energies, but drops at the threshold region.

The above effective couplings should be taken with cautions. In principle, the parametrization of the FF-I scheme contains all the contributions from the vector resonances, while FF-II contains only one resonance plus a background. By comparing these two form factors with each other, it would suggest the dominance of one single resonance around 3.94 GeV, which seems to support the need of $X(3900)$. However, it should be recognized that the Breit-Wigner structure fitted by the form factor is largely due to the collective contributions from nearby resonances such as $\psi(4040)$. The parametrization somehow tilts the resonance signal due to the unphysical background term. In fact, both Belle [18] and BABAR [33] observe the dominant $\psi(4040)$ in $e^+e^- \rightarrow D\bar{D}^* + c.c.$, but no signs for the $X(3900)$ there. This could, in fact, support that the enhancement at 3.9 GeV in $e^+e^- \rightarrow D\bar{D}$ is due to non-resonant mechanisms. For our purpose of extracting the effective $\gamma^* D\bar{D}^*(s)$ form factor, these parametrizations should be acceptable.

With the form factor coupling $g_{\gamma^* D\bar{D}^*}(s)$, we can then evaluate the $D\bar{D}^* + c.c.$ open channel effects in $e^+e^- \rightarrow D\bar{D}$. We plot the cross sections from the $D\bar{D}^*$ open channel in Fig. 8. As a comparison, we also include the Breit-Wigner form factor (solid line) for the $X(3900)$. Taking the cut-off parameter $\alpha = 2.0$, the dashed and dotted line are given by those two form factors, FF-I and FF-II, respectively. It shows that FF-I can lead to some enhancement to the cross sections below ~ 3.9 GeV, while the cross sections from these two form factors are similar to each other above 3.9 GeV. It shows that the behavior of the solid line is similar to FF-II except that the fitted mass and width are slightly different. The reason again should be that the fitted form factor FF-II contained all contributions from several nearby states. Thus, the fitted Breit-Wigner parameters contain unphysical information.

It is interesting to see that the cross section peaks from these different treatments are located in a similar place. In this sense, we argue that the present data cannot eliminate the possibility that the cross section enhancement at around 3.9 GeV could be from the $D\bar{D}^*$ open channel contributions.

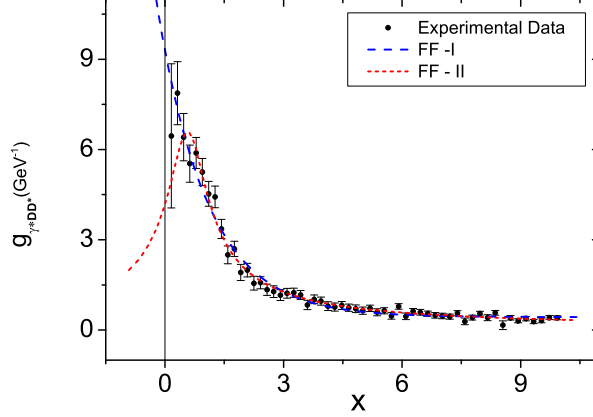


FIG. 7: The x -dependence of $g_{\gamma^* D \bar{D}^*}$ extracted from the cross sections for $e^+e^- \rightarrow D^+ D^{*-} + c.c.$ [18] with $x \equiv s - (m_D + m_{D^*})^2$. The dashed and dotted line are given by the FF-I and FF-II schemes, respectively. The vertical line at $x = 0$ labels the $D\bar{D}^*$ threshold.

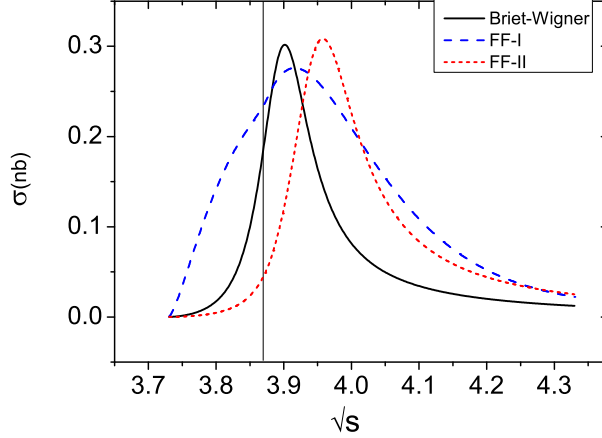


FIG. 8: The comparison of cross sections from different mechanisms around 3.9 GeV. The solid line is given by a Breit-Wigner resonance $X(3900)$ in Tab. II, while the dashed and dotted line are given by the FF-I and FF-II schemes, respectively. The vertical line labels the $D\bar{D}^*$ threshold. $\alpha = 2.0$ has been taken.

D. The ψ' - $\psi(3770)$ mixing results

Following the discussion of Sec. II C, we now investigate the energy-dependence of the mixing parameter $|\xi_i|$ defined in Eq. (17). As mentioned earlier that the s -dependence of the total widths is weak for both ψ' and $\psi(3770)$ near threshold, we thus keep the widths as constants. The $g_{\psi(3770) D \bar{D}}$ coupling appear to be different in the charged and neutral channel. Here for the purpose of investigating the energy-dependence of the mixing parameter, such a difference can be neglected. We then take $g_{\psi' D \bar{D}} = 9.05$ (the fitting results) and $g_{\psi(3770) D \bar{D}} = 12.66$ (the average obtained from Ref. [28]) to extract the mixing parameter $|\xi_i|$. The results are presented in Fig. 9.

The solid line denotes the mixing amplitude $|\xi_{\psi'}(s)| \equiv |D_{\psi'\psi(3770)}/D_{\psi'}|$, while the dashed line is for $|\xi_{\psi(3770)}(s)| \equiv |D_{\psi'\psi(3770)}/D_{\psi(3770)}|$. There are clear physical meanings for these two quantities. At a given energy \sqrt{s} , the value of $|\xi_{\psi'}(s)|$ denotes the coupling strength of the ψ' component inside an initial $\psi(3770)$ state (propagator), while $|\xi_{\psi(3770)}(s)|$ denotes the strength of the $\psi(3770)$ inside an initial ψ' state.

The mixing parameter $|\xi_{\psi'}(s)|$ at $\sqrt{s} = 3.773$ GeV can be related to the $\psi(2S)$ - $\psi(1D)$ state mixing

angle via $|\xi_{\psi'}(s)| \simeq |\sin \theta_{\psi'}|$ [13] for which we find $\theta_{\psi'} \simeq 5.4^\circ$. This value agrees with the one extracted in Ref. [5], although it is only about a half of the result estimated by Ref. [13]. It is worth emphasizing that this quantity strongly depends on the coupling strength of the $g_{\psi' D \bar{D}}$ coupling which is a consequence of the lineshape measurement of the cross sections near threshold. In this sense, the cross section for $e^+e^- \rightarrow D \bar{D}$ directly provides a constraint on the mixing angle.

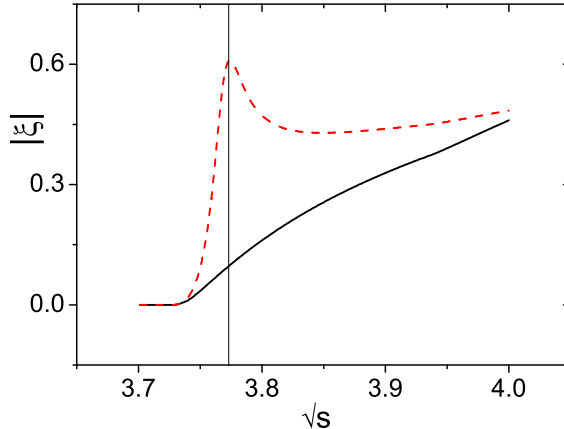


FIG. 9: The energy-dependence of the mixing parameter. The solid line is for $|\xi_{\psi'}(s)|$ while the dashed line for $|\xi_{\psi(3770)}(s)|$. The vertical line labels the $\psi(3770)$ mass position.

IV. SUMMARY AND DISCUSSION

In this work, we investigate the reaction mechanisms for $e^+e^- \rightarrow D \bar{D}$ from threshold to $\sqrt{s} \simeq 4.3$ GeV in an effective Lagrangian approach. We find that the cross section lineshape near threshold is very sensitive to the presence of ψ' . By fitting the cross sections from BES [2] and Belle [11], we succeed in extracting resonance parameters for ψ' , $\psi(3770)$, $X(3900)$ and $\psi(4040)$. It shows that coupling $g_{\psi' D \bar{D}}$ is consistent with those values given by other analyses. We show that it is important to have a reliable determination of this quantity, not only to understand the lineshape of the cross section at the mass of $\psi(3770)$, but also to provide a probe for the ψ' - $\psi(3770)$ state mixing.

The analysis also suggests a significant difference between $g_{\psi(3770) D^0 \bar{D}^0}$ and $g_{\psi(3770) D^+ D^-}$ which is quite different from the PDG averaged values [28]. In order to further clarify this, a precise measurement of both $D^0 \bar{D}^0$ and $D^+ D^-$ cross sections is strongly recommended, and BES-III would have great advantages on this issue [34].

We also study the $D \bar{D}^*$ open channel effects on the $e^+e^- \rightarrow D \bar{D}$ cross sections. We find that it cannot be eliminated that the enhancement at 3.9 GeV in the Belle data is due to the $D \bar{D}^*$ open channel contributions. Further investigation of this mechanism with more accurate data would be needed.

Acknowledgement

Useful discussions with Gang Rong and X.L. Wang are acknowledged. We thank Galina Pakhlova for useful comments on this work. This work is supported, in part, by the National Natural Science Foundation of China (Grants No. 10675131 and 10491306), Chinese Academy of Sciences (KJCX3-SYW-

N2), and Ministry of Science and Technology of China (2009CB825200).

-
- [1] M. Ablikim *et al.*, Phys. Rev. D **76**, 122002 (2007).
 - [2] M. Ablikim *et al.* [BES Collaboration], Phys. Lett. B **659**, 74 (2008).
 - [3] D. Besson *et al.*, Phys. Rev. Lett. **96**, 092002 (2006) [arXiv:hep-ex/0512038].
 - [4] Z. G. He, Y. Fan and K. T. Chao, Phys. Rev. Lett. **101**, 112001 (2008).
 - [5] Y. J. Zhang, G. Li and Q. Zhao, Phys. Rev. Lett. **102**, 172001 (2009) [arXiv:0902.1300 [hep-ph]].
 - [6] X. Liu, B. Zhang and X. Q. Li, Phys. Lett. B **675**, 441 (2009) [arXiv:0902.0480 [hep-ph]].
 - [7] S. Okubo, Phys. Lett. **5**, 165 (1963); G. Zweig, CERN Rep. 8419/TH-412; CERN Preprints TH-401, TH-412; J. Iizuka, Prog. Theor. Phys. Suppl. 37/38, 21 (1966).
 - [8] M. Ablikim *et al.* [BES Collaboration], Phys. Lett. B **668**, 263 (2008).
 - [9] M. Ablikim *et al.*, Phys. Rev. Lett. **101**, 102004 (2008).
 - [10] M. Z. Yang, Mod. Phys. Lett. A **23**, 3113 (2008) [arXiv:hep-ph/0610395].
 - [11] G. Pakhlova *et al.* [Belle Collaboration], Phys. Rev. D **77**, 011103 (2008) [arXiv:0708.0082 [hep-ex]].
 - [12] H. B. Li, X. S. Qin and M. Z. Yang, arXiv:0910.4278 [hep-ph].
 - [13] J. L. Rosner, Annals Phys. **319**, 1 (2005).
 - [14] E. Eichten, S. Godfrey, H. Mahlke and J. L. Rosner, Rev. Mod. Phys. **80**, 1161 (2008) [arXiv:hep-ph/0701208].
 - [15] T. H. Bauer, R. D. Spital, D. R. Yennie and F. M. Pipkin, Rev. Mod. Phys. **50**, 261 (1978) [Erratum-ibid. **51**, 407 (1979)].
 - [16] T. Bauer and D. R. Yennie, Phys. Lett. B **60**, 169 (1976).
 - [17] G. Li, Q. Zhao and B. S. Zou, Phys. Rev. D **77**, 014010 (2008) [arXiv:0706.0384 [hep-ph]].
 - [18] K. Abe *et al.* [Belle Collaboration], Phys. Rev. Lett. **98**, 092001 (2007) [arXiv:hep-ex/0608018].
 - [19] Y. J. Zhang, Q. Zhao and C. F. Qiao, Phys. Rev. D **78**, 054014 (2008) [arXiv:0806.3140 [hep-ph]].
 - [20] M. P. Locher, Y. Lu and B. S. Zou, Z. Phys. A **347**, 281 (1994) [arXiv:nucl-th/9311021].
 - [21] X. Q. Li, D. V. Bugg and B. S. Zou, Phys. Rev. D **55**, 1421 (1997).
 - [22] X. Q. Li and B. S. Zou, Phys. Lett. B **399**, 297 (1997) [arXiv:hep-ph/9611223].
 - [23] H. Y. Cheng, C. K. Chua and A. Soni, Phys. Rev. D **71**, 014030 (2005) [arXiv:hep-ph/0409317].
 - [24] R. Casalbuoni, A. Deandrea, N. Di Bartolomeo, R. Gatto, F. Feruglio, and G. Nardulli, Phys. Rep. **281**, 145 (1997).
 - [25] T. M. Yan, H. Y. Cheng, C. Y. Cheung, G. L. Lin, Y. C. Lin, and H. L. Yu, Phys. Rev. D **46**, 1148 (1992); **55**, 5851(E) (1997); M. B. Wise, Phys. Rev. D **45**, R2188 (1992); G. Burdman and J. Donoghue, Phys. Lett. B **280**, 287 (1992).
 - [26] N. N. Achasov, S. A. Devyanin and G. N. Shestakov, Phys. Lett. B **88**, 367 (1979).
 - [27] J. J. Wu and B. S. Zou, Phys. Rev. D **78**, 074017 (2008) [arXiv:0808.2683 [hep-ph]].
 - [28] C. Amsler *et al.* [Particle Data Group], Phys. Lett. B **667**, 1 (2008).
 - [29] A. Deandrea, G. Nardulli and A. D. Polosa, Phys. Rev. D **68**, 034002 (2003) [arXiv:hep-ph/0302273].
 - [30] R. D. Matheus, F. S. Navarra, M. Nielsen and R. Rodrigues da Silva, Phys. Lett. B **541**, 265 (2002) [arXiv:hep-ph/0206198].
 - [31] M. E. Bracco, M. Chiapparini, F. S. Navarra and M. Nielsen, Phys. Lett. B **605**, 326 (2005) [arXiv:hep-ph/0410071].
 - [32] Z. W. Lin and C. M. Ko, Phys. Rev. C **62**, 034903 (2000) [arXiv:nucl-th/9912046].
 - [33] B. Aubert *et al.* [BABAR Collaboration], Phys. Rev. D **79**, 092001 (2009) [arXiv:0903.1597 [hep-ex]].
 - [34] G. Rong, Talk on the 2009 Workshop on BES Physics, Huangshan, April 10-14, 2009.